



## Full Length Article

## Multi-stage model for the release of potassium in single particle biomass combustion

Andrés Anca-Couce<sup>a,\*</sup>, Peter Sommersacher<sup>b</sup>, Christoph Hochenauer<sup>a,b</sup>, Robert Scharler<sup>a,b</sup><sup>a</sup> Institute of Thermal Engineering, Graz University of Technology, Inffeldgasse 25b, 8010 Graz, Austria<sup>b</sup> BEST – Bioenergy and Sustainable Technologies GmbH, Inffeldgasse 21b, 8010 Graz, Austria

## ARTICLE INFO

## Keywords:

Potassium  
Release  
Biomass combustion  
Single particle  
Model

## ABSTRACT

The release of potassium during biomass combustion leads to several problems as the emissions of particle matter or formation of deposits. K release is mainly described in literature in a qualitative way and this work aims to develop a simplified model to quantitatively describe it at different stages. The proposed model has 4 reactions and 5 solid species, describing K release in 3 steps; during pyrolysis, KCl evaporation and carbonate dissociation. This release model is coupled into a single particle model and successfully validated with experiments conducted in a single particle reactor with spruce, straw and Miscanthus pellets at different temperatures. The model employs same kinetic parameters for the reactions in all cases, while different product compositions of the reactions are employed for each fuel, which is attributed to differences in composition. The proposed model correctly predicts the online release at different stages during conversion as well as the final release for each case.

## 1. Introduction

Biomass utilization for bioheat production is the main renewable energy use. In the EU-28, 88.5 Mtoe of bioheat were produced in 2017, which represented 7.6% of the total gross final energy consumption and almost the half of the renewable energy consumption in Europe [1]. Worldwide, bioheat production in 2017 was of 323 Mtoe from modern bioenergy and 660 Mtoe from traditional biomass utilization, which cannot be considered as renewable [2]. Nevertheless, the modern bioenergy use for bioheat represented 3.7% of the total gross final energy consumption and more than one third of the renewable energy consumption worldwide. Bioheat is mainly produced from combustion of solid biomass [1,2] which is an established technology. Over 50% of bioheat is directly consumed in the residential sector in Europe [3], primarily by small scale combustion devices. Industry and district heat are the other two relevant bioheat sectors, being larger scales commonly employed and, in some cases, coupled with power production. In addition, due to the need to significantly reduce CO<sub>2</sub> emissions, the combustion of biomass for bioheat generation is expected to increase in the following years [1,2].

In modern automatic biomass combustion devices operated with solid biomass, the emissions of unburnt products, including CO, organic gaseous compounds (OGC) or soot are minor. The emissions with a higher environmental impact are nitrogen oxides (NO<sub>x</sub>) and particle

matter (PM) [4–6]. PM emissions for modern automatic biomass combustion are mainly inorganic and composed of alkali chlorides, sulfates and carbonates which nucleate in the gas phase after the release of alkalis, chloride and sulfur from the fuel bed [5,7,8]. Besides heavy metals, the alkali content in a biomass fuel [9] or the content of alkalis, sulfur and chloride [10] are appropriate predictors of the PM emissions. The main alkali metal in biomass is potassium (K) [11], but it is present at different concentrations. Combustion of herbaceous and agricultural biomass leads commonly to higher PM emissions than woody biomass, because they have a higher alkali content and therefore a higher release of alkali metals leading to PM emissions [9]. For all cases, PM emissions should be minimized. For small-scale applications, secondary measures are commonly too expensive, so these emissions should be reduced by primary measures. For larger scales, PM emissions can be reduced with e.g. electrostatic precipitators, but the release of alkalis can lead as well to other problems, such as the formation of deposits leading to fouling or slagging as well as corrosion if chlorine is also present [8,12]. Therefore, it is crucial to reduce the K release from the bed in biomass combustion.

Potassium is a main macronutrient for biomass and it is mainly present in the inorganic fraction as a water-soluble salt [13]. K can be released at high temperatures and the mechanisms of K conversion have been discussed by several authors, including the release at several stages [14,15,16,17] or phenomena as agglomeration [18,19].

\* Corresponding author.

E-mail address: [anca-couce@tugraz.at](mailto:anca-couce@tugraz.at) (A. Anca-Couce).<https://doi.org/10.1016/j.fuel.2020.118569>

Received 8 May 2020; Received in revised form 25 June 2020; Accepted 29 June 2020

Available online 09 July 2020

0016-2361/ © 2020 The Author(s). Published by Elsevier Ltd. This is an open access article under the CC BY license

<http://creativecommons.org/licenses/by/4.0/>.

However, K release is not yet fully understood and the descriptions of the process available with the current understanding are mainly qualitative [20]. The objective of this work is to develop a simplified model which describes it quantitatively.

During pyrolysis, a fraction of K can be released to the gas phase. However, the most significant fraction of K is bound to the char after pyrolysis, mainly in carboxyl groups and, at higher temperatures, in phenolic groups or intercalated [15]. Other critical elements for PM formation such as chlorine or sulfur are already released to a significant extent (usually  $\geq 50\%$ ) at temperatures lower than  $500\text{ }^{\circ}\text{C}$  [21]. For K, the release in pyrolysis for temperatures up to  $700\text{ }^{\circ}\text{C}$  is usually limited to low percentages for several biomasses [22,23,24,25], except when extremely low bed heights and high gas flow rates are employed [26,27,28]. At higher temperatures, the remaining chlorine is typically bound with K and this salt can evaporate [24,29]. Furthermore, char conversion takes place during biomass combustion, producing the ashes. K is retained to a significant extent in the ashes, mainly in (alumino-)silicates [30] which are stable at the high temperatures that are typically achieved in biomass combustion. K is also present as a carbonate ( $\text{K}_2\text{CO}_3$ ) or sulfate ( $\text{K}_2\text{SO}_4$ ), which can lead to the release of K at high temperatures due to their dissociation or evaporation [25]. The total K release depends on the biomass composition, as e.g. a high silicon concentration decreases the release, retaining K in silicates, while a higher chlorine concentration increases it, releasing K as KCl. Temperature plays as well a crucial factor in determining the total K release [15] and it was shown that cooling the fuel bed reduces the K release, leading to lower PM emissions [31].

Previous works have attempted to model K release. However, this was conducted with a single Arrhenius reaction to describe the release in biomass combustion [32,33] or only during biomass pyrolysis with several [29] or one [34] reactions. However, as previously reviewed, K release takes place at different steps. In this work a simplified scheme including the most relevant steps of K release is proposed. The model will be validated with experimental data from single particle experiments. The experimental setup will be described in Section 2 and the employed models in Section 3. The results and discussion are presented in Section 4 and finally the conclusions are exposed.

## 2. Experimental setup

Experiments were conducted with a single particle reactor. The reactor setup was described in [35]. Experimental results with spruce pellets and wheat straw pellets in an oxidizing atmosphere at  $700$ ,  $850$  and  $1000\text{ }^{\circ}\text{C}$  were published in a journal paper [36] and with Miscanthus pellets in a conference proceeding [37]. In this work these results are analyzed together and employed for model validation, considering in this way representative fuels for woody (spruce), herbaceous (Miscanthus) and agricultural (straw) biomasses, which are the main groups of solid lignocellulosic biomass. Two different batches were employed for spruce pellets, one for the experiments at  $700\text{ }^{\circ}\text{C}$  and another one for the experiments at  $850$  and  $1000\text{ }^{\circ}\text{C}$ . The fuel composition is detailed in Table 1. The obtained values are representative for each case. For spruce, the minor element with a higher concentration is Ca, followed by K, while for straw and Miscanthus it is Si, followed by K. The properties of the cylindrical pellets are detailed in Table 2 for each case as well as the employed oxygen content in the oxidizing atmosphere.

Two different types of experiments were conducted for each fuel and temperature: until a complete conversion was achieved and no more K release is detected, leaving only the ashes as a solid product, and until a quench point which was selected for each case after the main devolatilization phase. In the last case – quench experiments – the experiment is interrupted at a certain time (shown in Table 3) and the pellet on the sample holder is flushed with  $\text{N}_2$ . In order to determine the quench point, the tests without quench (complete experiments) were carried out first. The time at which the  $\text{CO}_2$  concentration drops to  $<$

$0.2\%$  vol. after passing through the maximum in the complete experiments was selected as the quench point. More details about the quench procedure can be found in [35]. For all experiments the online release data for S, Cl, K, Na, Zn and Pb was obtained with an inductively coupled plasma mass spectrometer (ICP-MS). Besides, the mass loss and the temperatures in the center and surface of the particle were measured as described in [35].

The total mass and K, Cl and S contents were measured in the initial fuel as well as in the ashes after the complete experiments and in the solid residue (mainly char) after the quench experiments. The K, Cl and S releases can be then determined after sampling at these 2 points (quench and complete). Moreover, the ICP-MS signal from the complete experiments was employed to determine the online K release between the beginning of the experiments and quench point as well as between the quench point and the complete experiment. Actually, the quench experiments are conducted to have a reliable measurement of the release until this point, as the mass and K release rates are higher before this point than after it. For each case, 3 repetitions were conducted. A good reproducibility was obtained for most of the cases. For the ICP-MS signal the only exceptions were the cases with spruce at  $700\text{ }^{\circ}\text{C}$ , where K release was detected online only for one of the three repetitions, and with spruce at  $1000\text{ }^{\circ}\text{C}$ , where K release after the quench point was as well only detected in one case. These single particle experiments are described with a single particle model coupled to a K release model, which are explained in detail in the next section.

## 3. Models

### 3.1. K release model

The simplified release model is shown in Fig. 1 and it includes the main steps for K release, which were presented in the introduction. During pyrolysis (R1), a fraction of the K from the fuel is released (K-gas). The combined release of K to the gas phase during pyrolysis is described in the model, without specifying if this release takes place as K, KOH or KCl. The main fraction of K is however retained in the solid after pyrolysis. The remaining Cl in the solid at this point will be bound with K as KCl (K-KCl), while the other K fraction after pyrolysis is directly bound with the char (K-char). KCl evaporation (R2) can take place at high temperatures releasing K to the gas phase. Furthermore, after char conversion (R3), K can be retained in the ashes (K-ash), mainly as (alumino)silicates, or be present in carbonates ( $\text{K}_2\text{CO}_3$ ), which can dissociate (R4) further releasing K to the gas phase. The formation of sulfates is not considered in this simple model, as sulfates can lead to K release at higher temperatures ( $> 1000\text{ }^{\circ}\text{C}$ ) than the ones experimentally investigated in this study [25]. Besides, the S content is significantly lower than the K content for the investigated fuels and S is mainly released during pyrolysis.

The product distribution in mass fraction employed in the model for the pyrolysis (R1) and char conversion (R3) reactions is shown in Table 4. The values are different for each fuel due to their different elemental composition which, as previously commented, influences the release behavior. In the pyrolysis reaction (R1) there are three products: K-gas, K-KCl(s) and K-char(s). The K-gas fraction is taken from the average K release until the quench point for the experiments described in section 2 at  $700$  and  $850\text{ }^{\circ}\text{C}$ , which is quite similar for both temperatures, because the K release in this first stage is dominated by pyrolysis as it will be shown when presenting the modelling results. The remaining Cl after the quench point (on average  $15\%$  of the initial Cl content for all temperatures) is assumed to be bound as KCl. The remaining K fraction after pyrolysis is assumed to be present as K-char. In the char conversion reaction (R3) there are two products: K- $\text{K}_2\text{CO}_3$ (s) and K-ash(s). The fraction of carbonate formation (K- $\text{K}_2\text{CO}_3$ ) in R3 is selected to match the final total release of K for each fuel. The release depends on temperature and carbonate dissociation will take place to a different extent with variations in temperature. The remaining K from

**Table 1**  
Composition of the employed fuels.

			Spruce 850, 1000 °C	Spruce 700 °C	Miscanthus	Straw
Ash content		% mass d.b.	0.40	0.34	2.6	4.5
Moisture		% mass w.b.	8.8	7.7	8.2	13.5
Carbon	C	% mass d.b.	50.2	49.8	48.0	46.6
Hydrogen	H	% mass d.b.	6.2	6.3	6.0	6.0
Nitrogen	N	% mass d.b.	0.05	0.07	0.33	0.40
Sulfur	S	mg/kg d.b.	72	68	432	913
Chlorine	Cl	mg/kg d.b.	59	36	902	2 300
Silicon	Si	mg/kg d.b.	420	94	4 970	11 100
Calcium	Ca	mg/kg d.b.	751	927	2 380	3 010
Magnesium	Mg	mg/kg d.b.	140	130	601	688
Aluminium	Al	mg/kg d.b.	34	19	130	217
Iron	Fe	mg/kg d.b.	97	27	834	173
Manganese	Mn	mg/kg d.b.	82	111	30	22
Phosphorus	P	mg/kg d.b.	44	41	886	385
Potassium	K	mg/kg d.b.	564	412	4 810	6 970
Sodium	Na	mg/kg d.b.	22	18	144	201
Cooper	Cu	mg/kg d.b.	1.1	1.0	2.5	2.0
Zinc	Zn	mg/kg d.b.	13	11	21	6.6
Lead	Pb	mg/kg d.b.	0.2	0.2	0.5	0.2
Cadmium	Cd	mg/kg d.b.	0.1	0.2	0.5	0.1

**Table 2**  
Pellet properties and oxygen content in the employed atmosphere for each case.

Property	Unit	Spruce 850, 1000 °C	Spruce 700 °C	Miscanthus	Straw
Diameter	mm	8	8	8	8
Length	mm	19	19	21	21
Dry density	kg/m <sup>3</sup>	1050	1120	1000	950
O <sub>2</sub> content	% vol.	5.6	4.2	5.6	5.6

**Table 3**  
Duration (s) of the quench experiments for each case, selected after the main devolatilization phase. The complete experiments were conducted until only ashes were left as a residue and no more K release is detected.

	Spruce	Miscanthus	Straw
700 °C	145	129	95
850 °C	90	100	85
1000 °C	76	73	59

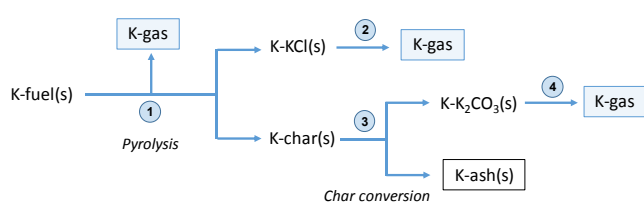


**Fig. 1.** Simplified scheme for K release. Reactions: R1 – pyrolysis, R2 – KCl evaporation, R3 – char conversion, R4 – carbonate dissociation.

**Table 4**  
Product distribution in mass fractions of K employed in the model for the pyrolysis (R1) and char conversion (R3) reactions.

	Pyrolysis (R1)			Char conversion (R3)	
	K-gas	K-KCl(s)	K-char(s)	K-K <sub>2</sub> CO <sub>3</sub> (s)	K-ash(s)
Spruce	0.080	0.015	0.905	0.25	0.75
Miscanthus	0.050	0.030	0.920	0.09	0.91
Straw	0.050	0.055	0.895	0.15	0.85

char conversion is bound in the ashes (K-ash). The employed values shown in Table 4, which are indirectly derived from the experiments as previously explained, are in accordance to the fuel composition shown

in Table 1. Spruce, with the lowest Cl/K and Si/K ratios, has the lowest formation of K-KCl in R1, due to a low Cl content, and of K-ash in R3, due to a low Si content leading to a lower K retention in silicates. The suitability of the employed values to describe the release at different conditions will be discussed in the next section. The other two reactions, KCl evaporation (R2) and carbonate dissociation (R4), have only one product.

The pyrolysis (R1), KCl evaporation (R2) and carbonate dissociation (R4) reactions are modelled as Arrhenius first order reactions with kinetics parameters shown in Table 5. The same kinetic values are employed for all fuels. For the char conversion reaction (R3) no kinetics are needed, as it is described by the single particle model which will be later introduced. The pyrolysis reaction (R1) describes the online K release during the first stage of the experiment. The employed activation energy for this reaction (190 kJ/mol) is selected to be similar to other activation energies in literature for K release in pyrolysis [29,34] and the pre-exponential factor is selected to correctly describe the online release in the first stage of the experiments. The employed values are discussed in the next section.

The kinetics employed for the K release in reactions R2 – KCl evaporation ( $KCl_{(s,l)} \rightarrow KCl_{(g)}$ ) and R4 – K<sub>2</sub>CO<sub>3</sub> dissociation ( $K_2CO_{3(s,l)} + H_2O_{(g)} \rightarrow 2 KOH_{(g)} + CO_{2(g)}$ ) are approximated from a simple model based on equilibrium calculations, which describes the release of KCl or KOH at different temperatures. It is assumed in this simple model that for a sample at a certain temperature the equilibrium vapor pressure in each reaction is equal to the partial pressure close to the sample of the released compound, as in a closed system. It is considered that there are no mass transfer limitations for the release from the sample to the environment and that the partial pressure of the released compounds in the environment is zero. The mass release of KCl or KOH is therefore estimated as shown in Eq. (1) [25]; being  $p_{eq,i}$  the equilibrium vapor pressure of KCl evaporation or K<sub>2</sub>CO<sub>3</sub> dissociation,  $M_i$  the molecular mass of KCl or KOH,  $R_{gas}$  the gas constant and T the temperature. The equilibrium vapor pressure  $p_{eq,i}$  is directly calculated

**Table 5**  
Activation energies (E) and pre-exponential factors (A) for Arrhenius reactions in K release model.

	E (kJ/mol)	A (1/s)
Pyrolysis (R1)	190	5.0e9
KCl evaporation (R2)	175	5.0e5
Carbonate dissociation (R4)	266	400 * 5.0e5

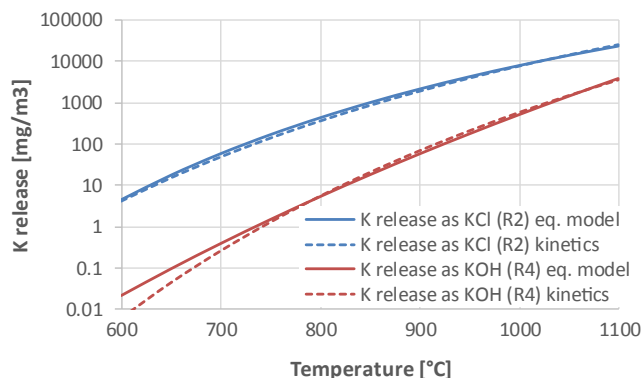


Fig. 2. Release of K as KCl from KCl evaporation (R2) and as KOH from  $K_2CO_3$  dissociation (R4) calculated with the simple equilibrium model and the employed kinetics (note: the pre-exponential factors in Table 5 kinetics are multiplied by a factor with units of  $m^3/(mg*s)$ ).

from the equilibrium constant for KCl evaporation, while for  $K_2CO_3$  dissociation it is calculated from Eq. (2), being  $K_{eq}$  the equilibrium constant and  $p_{amb}$ ,  $p_{CO_2}$  and  $p_{H_2O}$  the ambient as well  $CO_2$  and  $H_2O$  partial pressures. It is assumed an ambient pressure of 1 bar and that the  $CO_2$  concentration inside the particle is ten times higher than the  $H_2O$  concentration, based on simulations of char conversion with the single particle model. The equilibrium constant  $K_{eq}$  is calculated as shown in Eq. (3) from the difference in Gibbs energy of reactants and products ( $\Delta G_r$ ), obtained from the NIST-JANAF database [42].

$$Release_i = \frac{p_{eq,i} M_i}{R_{gas} T} \quad (1)$$

$$p_{eq,K_2CO_3} = \sqrt{2K_{eq} p_{amb}^2 \frac{p_{CO_2}}{p_{H_2O}}} \quad (2)$$

$$K_{eq} = \exp(-\Delta G_r/RT) \quad (3)$$

The release of K as KCl from KCl evaporation (R2) and of K as KOH from carbonate dissociation (R4) calculated with Equation (1) based on the equilibrium model is shown in Fig. 2 at different temperatures. This release behavior is described in the K release model with Arrhenius reactions representing it, which facilitates the integration into single particle models. The employed kinetic parameters are shown in Table 5. The activation energies can correctly describe the influence of temperature shown in Fig. 2, for the whole range of the figure for KCl evaporation and for temperatures higher than 800 °C (which is the range of interest, as it is extremely low at lower temperatures) for  $K_2CO_3$  dissociation releasing KOH. Besides, the pre-exponential factor from  $K_2CO_3$  dissociation should be 400 times higher than for KCl evaporation to reproduce the results of Fig. 2. The releases calculated in Fig. 2 have the units of  $mg/m^3$ . The pre-exponential factors finally employed in the single particle model and shown in Table 5 have units of  $1/s$ . They are obtained from the ones of Fig. 2 multiplied by a certain factor with units of  $m^3/(mg*s)$  to consider that the release also depends on the area and mass transport phenomena in the single particle. This factor is assumed to be the same for both reactions and is selected to match the final total release of K for each temperature. Therefore, the pre-exponential factors of the kinetic reactions in Table 5 keep the same ratio, i.e. it is 400 times higher for carbonate dissociation than for KCl evaporation. The employed values for these reactions will be as well discussed in the next section.

### 3.2. Single particle model

The single particle model is a volumetric one-dimensional model which describes the transport of mass and energy as well as chemical reactions inside the particle. The model has been initially developed to

describe pyrolysis with a simple pyrolysis scheme [38] and was later extended to describe drying and char oxidation during conversion of single pellets [39] and of a large wood log [40]. Drying and pyrolysis are described each one with a single Arrhenius reaction, and the product composition of pyrolysis is derived from a detailed pyrolysis scheme, the RAC scheme [41]. Char oxidation is described with surface kinetics and the suitable  $CO/CO_2$  ratio obtained during char conversion was derived in [39]. Other model properties are as described in [38,39,40], where further information can be found.

The model is applied for cylindrical pellets with the properties shown in Table 2. The initial moisture and ash contents of each pellet are shown in Table 1. Experiments are modelled at reactor temperatures of 700, 850 and 1000 °C. The experiments are conducted in an oxidizing atmosphere obtained from a mixture of air and nitrogen leading to the oxygen concentrations shown in Table 2 and with flow velocities of 0.416, 0.480 and 0.544 m/s for the experiments at 700, 850 and 1000 °C, respectively.

## 4. Results and discussion

### 4.1. Release in single particle experiments

The release of K, Cl and S in the single particle experiments is shown in Fig. 3 for the quench and complete experiments. The experiments were conducted in an oxidizing atmosphere with a relatively low oxygen content of around 5% vol. (see Table 2), which is a typical condition for biomass conversion in a fuel bed at staged combustion. The release generally increases with the temperature, but there are significant differences for each compound and fuel. The release in the first stage until the quench point, where mainly pyrolysis takes place, is limited for K, with values lower than 12% for all cases. Higher K releases are achieved for the complete experiments, including also the char conversion stage, especially at higher temperatures. The K release for the complete experiment significantly increased at the highest temperature for spruce, while this increase with temperature was more moderated for straw and Miscanthus.

For Cl, significantly higher releases were achieved. An almost complete release was achieved for the complete experiments, even for the cases at 700 °C, and most of it took place already during the first stage, until the quench point. A detailed analysis shows that a higher amount of Cl in mols was released than for K until the quench point, especially for straw and Miscanthus (with a higher Cl content) and to a higher extent at 700 and 850 °C. This supports that Cl release takes place to a significant extent at this first stage not bound with K, within compounds as  $CH_3Cl$  [21]. For S, a significant but not complete release was achieved, indicating that sulphates may have remained in the final ash. Most of the S release took place during the first stage until the quench point. For lower temperatures, at 700 and 850 °C, the S release after the quench point was generally extremely low whereas at 1000 °C it was significant.

The measured online K release is shown in Fig. 4 together with mass loss for the case of Miscanthus at 1000 °C as an example of the typical online behavior. The initial devolatilization phase where most of the mass loss takes place is fast. At this stage there is also a significant release of potassium, which starts later than the mass loss. The quench point is selected at a time (73 s, see Table 3) where the main devolatilization has already ended. Afterwards char combustion takes place, leading to a slower mass loss rate. This last stage is considerably longer and K release is also significant although it takes place at a slower rate. The other cases also follow this general behavior. The online release of K is shown in Fig. 5 for all cases together with a comparison with the model. This comparison between experiments and model predictions is discussed in the next section.

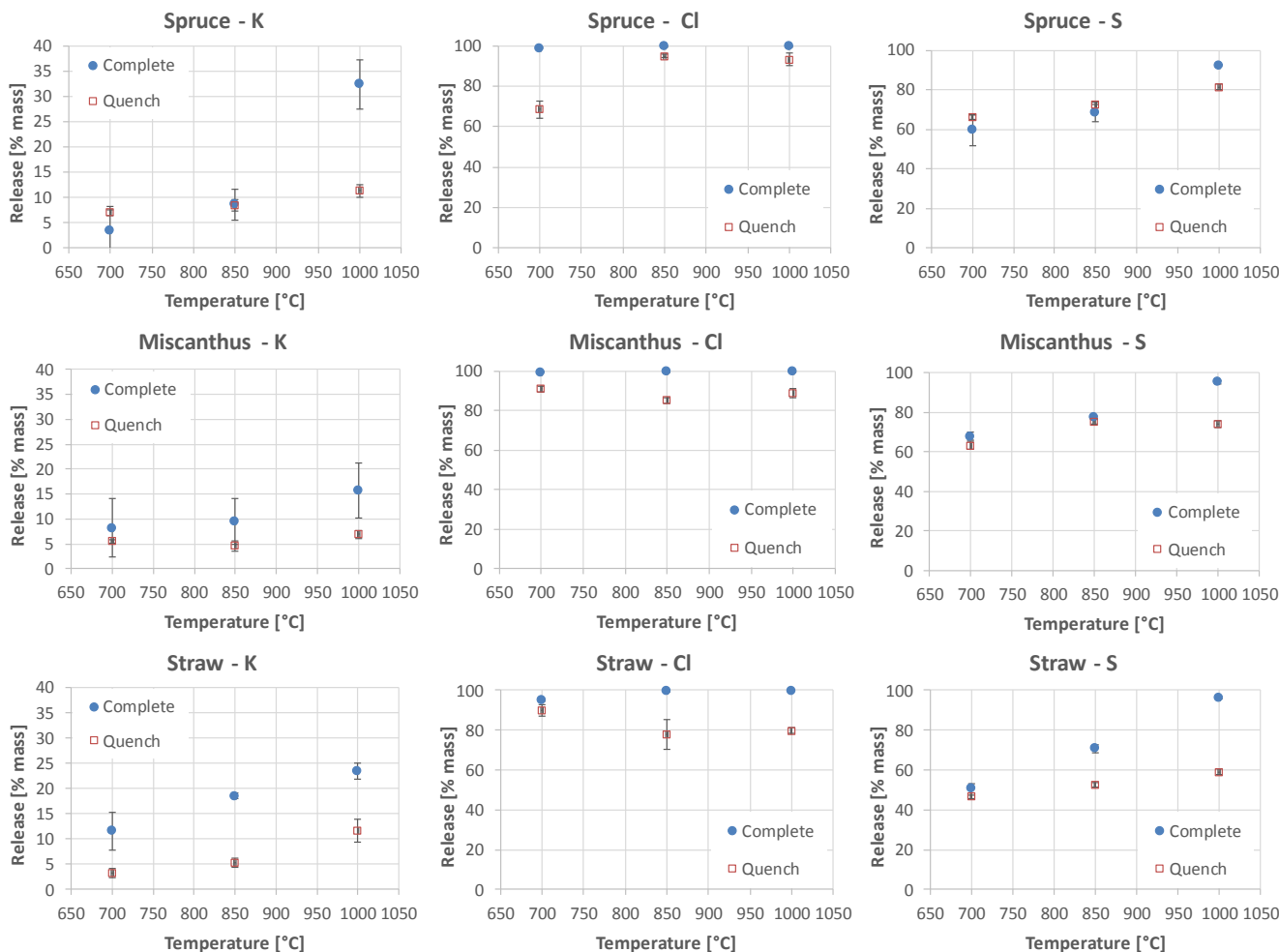


Fig. 3. Release in percentage of K, Cl and S in single particle experiments for the complete and quench experiments employing spruce, Miscanthus and straw at different temperatures.

4.2. Application of K release model

The novel K release model was applied together with the single particle model described in Section 3 and the results were compared with the experiments explained in the previous section. This comparison is shown in Fig. 5 for all cases, including the model results as well as the measured online K release and the points where sampling was performed (quench and complete experiment). The quench point was selected after the initial devolatilization stage and the experiment is considered complete when the measured temperatures in the particle achieve the target final temperature after the exothermic char conversion stage. At this stage no more K release has been detected online by

ICP-MS for all cases, except for spruce at 1000 °C. In the latter case it is considered that the experiment is completed when no more K release was detected. There is generally a good prediction with the K release model of the online release behavior and the final total releases which were measured experimentally.

For a better understanding of the model features, the evolution of K in different compounds is also shown in Fig. 6 for Miscanthus. K release to the gas phase (K-gas) takes place according to the model through 3 different ways (see Fig. 1): during pyrolysis, KCl evaporation and carbonate ( $K_2CO_3$ ) dissociation. Pyrolysis is the first reaction and it takes place at the beginning of the experiment. After this reaction the K which was initially in the fuel (K-fuel) is mainly bound to char (K-char)

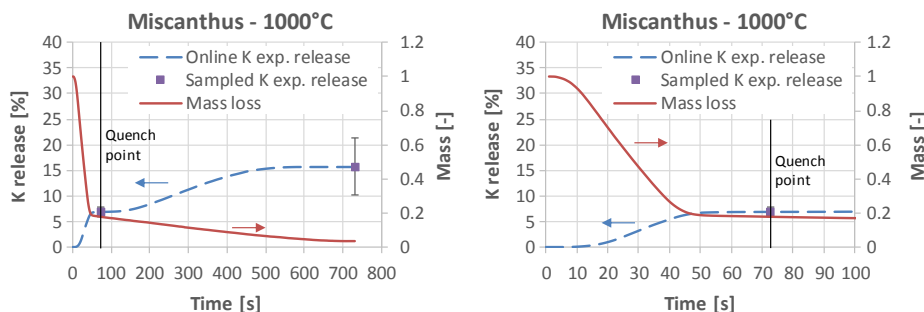


Fig. 4. Online K release measured experimentally, including the release at the sampling points (quench and complete experiments) and mass loss for the case of Miscanthus at 1000 °C during the whole experiment (left) and the initial 100 s (right).

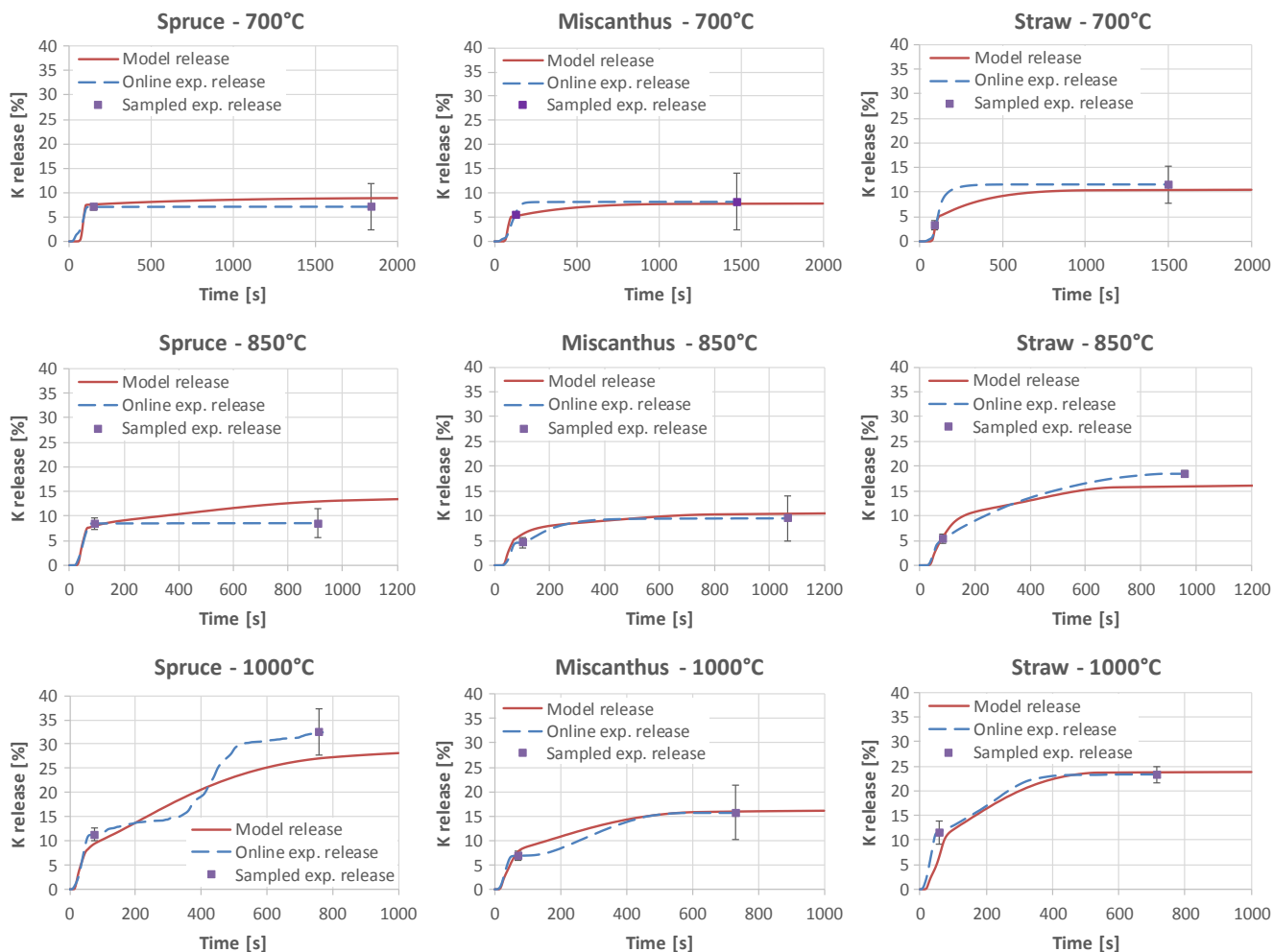


Fig. 5. Release of K during the complete experiments predicted by the model and experimentally measured, including the online measurements and the sampled points (quench and complete experiments).

(see Fig. 6), but there is also a significant fraction which is already released to the gas phase (K-gas) as well as a fraction bound to Cl (K-KCl). This release of K during pyrolysis is the main responsible for K release before the quench point. After pyrolysis, the possible K releases are due to KCl evaporation or the dissociation of  $K_2CO_3$  which is formed during char conversion. According to the model, KCl evaporation takes place at a slow pace for the experiment 700 °C (see Fig. 6) and it is much faster at 1000 °C. However, in all cases the content of KCl is close to zero at the end of the experiment, which is consistent with the experimentally measured Cl release close to 100% (see Fig. 3). This is not the case for the carbonate dissociation reaction.  $K_2CO_3$  is formed from char conversion (although the main product is K bound to the ashes) and its dissociation is almost complete for the experiment at 1000 °C (see Fig. 6), but it takes place to almost no extent for the experiment at 700 °C. At the end of conversion most of the K is bound to the ashes (K-ash), but for the cases at a temperature of 850 °C and specially 700 °C some K is still present as a carbonate, leading to a lower K release and higher retention in these cases. For other fuels, the general trends are the same as for Miscanthus, due to the same kinetics are employed for all cases, but there are differences in the proportions of the individual K compounds. The biggest difference among fuels is the higher proportion of carbonates in wood (spruce), which increases the release at the highest temperature.

The proposed model can describe with a good accuracy the K release in most of the experiments of all fuels. It can describe the initial release at a high rate during pyrolysis and the increase in release at higher temperatures due to the carbonate dissociation reaction taking place to

a higher extent. The biggest differences between model and experiments are for the cases at 700 °C for all fuels and for spruce at all temperatures. It should be noted that these are the cases where the K release is the lowest, due to the low K concentration in spruce and the lower release at 700 °C for all fuels. In these cases, the model predicts a K release to a lower extent than in the experiments immediately after the quench point and a continuous release until the end of the experiment which has not been experimentally detected. The deviations are however not high. The main exception is the case for spruce at 1000 °C, where the release significantly increases at this temperature due to the higher proportion of carbonates for this fuel. The increased release is well predicted by the model, but there are discrepancies in the online release. It should be noted, however, that this was one of the only two cases (see Section 2) where a reproducibility could not be achieved by the ICP-MS signal of the online release, as K release was only detected after the quench point in one of the three conducted experiments with spruce at 1000 °C. Therefore, the deviations may also arise due to the uncertainty in the measurement. Considering all cases and that certain deviations are only present when K release takes place to a low extent, it can be concluded that the employed product distribution of the reactions as well as kinetics for the KCl evaporation and  $K_2CO_3$  dissociation are suitable to describe these single particle experiments.

For analyzing in more detail the initial release during the devolatilization stage, the results are plotted for all cases during the first 160 of each experiment in Fig. 7. The K release during this initial stage is dominated by the pyrolysis reaction. It should be noted, however, that this K-pyrolysis reaction is not equivalent to a reaction describing

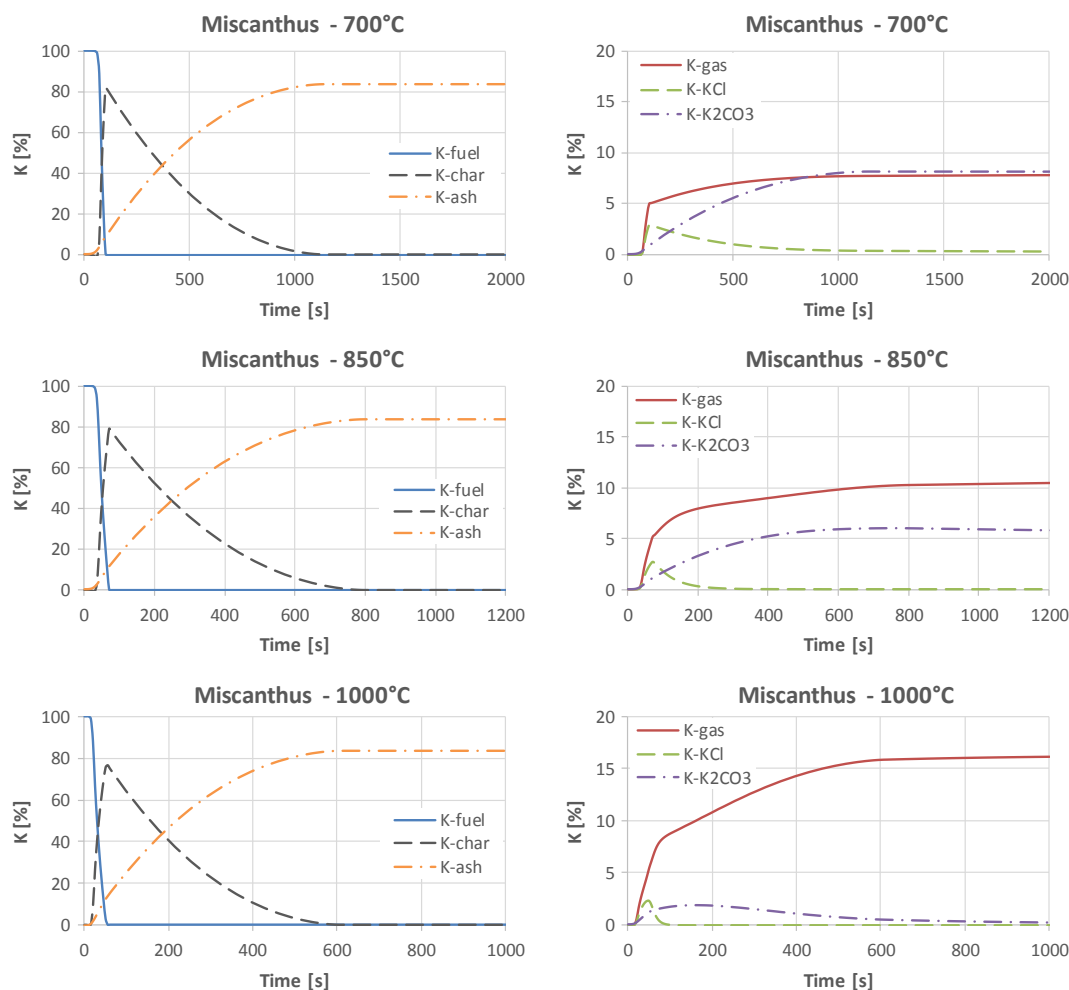


**Fig. 6.** Model results for the K distribution as percentage of the initial quantity in the fuel present in the fuel, char and ash (left) as well as present as KCl or K<sub>2</sub>CO<sub>3</sub> in the solid phase and released to the gas phase (right) during conversion for Miscanthus at different temperatures.

lignocellulosic biomass pyrolysis. K release is delayed in comparison to mass loss. For example, for Miscanthus at 1000 °C the mass loss is already significant at the beginning (see Fig. 4) while the K release starts at around 20 s, where around 30% of the mass loss took already place. The start of the K release, determined by the pyrolysis reaction (see Fig. 1), is well described for most of the cases. The deviations are also higher at 700 °C, especially for spruce, where the K release is lower and a reproducibility could not be achieved by the ICP signal of the online K release (see Section 2), and also for straw at 1000 °C, where the measured release takes place before the model predictions, without a clear explanation for this phenomenon.

The kinetics within this work are compared with other literature works. Fatehi et al. experimentally derived with cylindrical wood particles (8 mm diameter and 4 mm height) an activation energy for K release of 185 kJ/mol during the initial pyrolysis stage (168–198 kJ/mol) [34] and in another work with the same biomass an activation energy of 266 kJ/mol (238–292 kJ/mol) during char conversion [32]. Zhang et al. [33] obtained with small samples (20–50 mg) of pine wood an activation energy of 89.9 kJ/mol for K release during complete conversion, being mainly linked to carbonate dissociation. Olsson et al. [29] employed 20 mg of wheat straw and obtained during pyrolysis activation energies of  $156 \pm 11$  and  $178 \pm 8$  kJ/mol in the two main K release peaks at temperatures lower than 500 °C, and in the range of 168–238 kJ/mol (average of 197 kJ/mol) for different straw samples at higher temperatures. The high temperature release of Olsson et al. was more relevant and related to KCl evaporation. In this work, the activation energy for pyrolysis is selected (190 kJ/mol) similar than in

previous literature works (Olsson et al. [29] and Fatehi et al. [34]) and the pre-exponential factor is optimized to correctly describe the experiments. As shown in Fig. 7, most of the cases can be described with a good accuracy with these pyrolysis kinetic values. The values derived in this work for KCl evaporation (175 kJ/mol) are similar to the values associated to it by Olsson et al. [29]. For carbonate dissociation (266 kJ/mol), dominating during the char conversion stage, the value is the same as the one that Fatehi et al. [32] obtained for this last stage, although different to the one of Zhang et al. [33]. There are however significant differences in the pre-exponential factor for pyrolysis and carbonate dissociation of this work and the ones of Fatehi et al. [32,34].

The derived model is a step forward compared to previous works as it proposes a mechanism with different reactions to describe K release at several stages. The selected activation energies for each reaction are consistent with previous research. Furthermore, the novel model can describe K release for several fuels at different temperatures employing the same kinetics for all cases, with only modifications in the product distribution of the reactions for each fuel due to their different composition. There are however some limitations. The model is simplified, e.g. the pyrolysis release is modeled with only one reaction or the release from sulfates is not included which would be relevant for fuels with a high S content and at high temperatures. Besides, it has been validated for experiments with single pellets, while the release may change for smaller particles, as stated in the introduction for pyrolysis, or depending on the bed configuration, as the released K could be re-condensed in the bed [43] or the presence of more oxidizing or reducing conditions can affect the release. In addition, the product

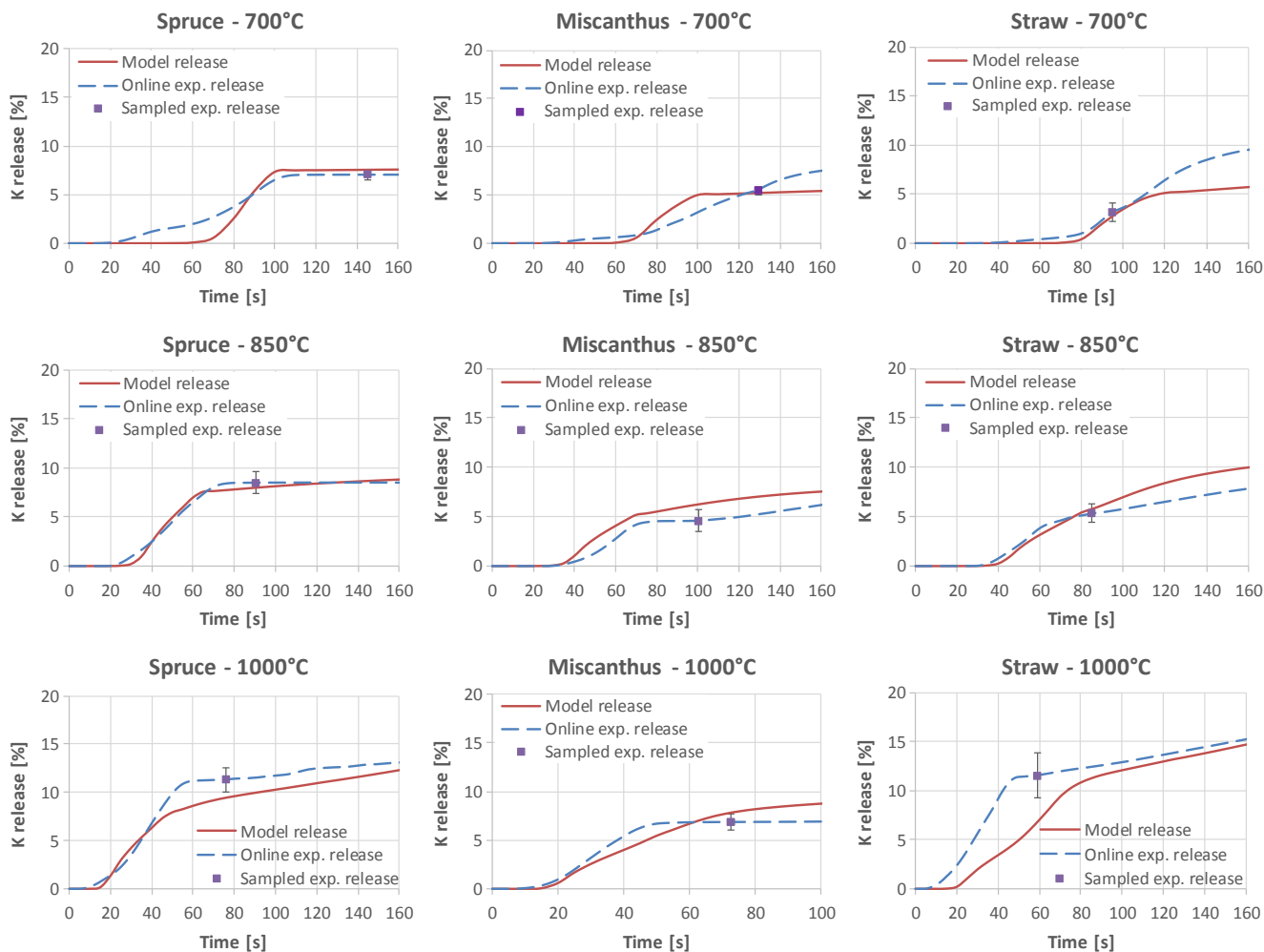


Fig. 7. Release of K predicted by the model and experimentally measured, including the online measurements and the sampled point (quench), during the first part of the experiments (up to 160 s) where the main the devolatilization phase takes place.

distribution of the reactions is assigned based on the experiments and not derived via the model, which would be a challenging task due to the complexity of the interactions between the ash-forming elements that influences the K release [44]. However, this product distribution for a certain fuel could be approximated on a first approach from fuels of similar elemental compositions. Generally, fuels with a high chlorine content would have a higher production of KCl from pyrolysis and fuels with a higher silicon content would have a higher production of carbonates from char conversion and therefore a lower K retention in silicates. Despite these limitations, this model is a relevant advance in order to quantitatively describe the K release of several fuels.

## 5. Conclusions

The release of K from single particle experiments of spruce, straw and Miscanthus pellets at different temperatures was described with a simple K release model with 4 reactions coupled with a single particle model. The model successfully predicts the K release at different stages of the process, describing it during pyrolysis, KCl evaporation and carbonate dissociation. The model employs the same kinetic parameters for the reactions in all cases with different temperatures and fuels, while for each fuel different product compositions of the reactions are used due to variations in composition. The model predicts with a good accuracy the final release at different temperatures and the online evolution of the release, with the largest deviations in cases with a low K release. This is therefore a relevant contribution to quantitatively

predict the K release during biomass conversion for several cases.

## CRedit authorship contribution statement

**Andrés Anca-Couce:** Conceptualization, Formal analysis, Writing - original draft. **Peter Sommersacher:** Investigation, Resources, Writing - review & editing. **Christoph Hochenauer:** Supervision, Writing - review & editing. **Robert Scharler:** Supervision, Writing - review & editing.

## Declaration of Competing Interest

The authors declare that they have no known competing financial interests or personal relationships that could have appeared to influence the work reported in this paper.

## Acknowledgment

The financial support of the Austrian Federal Government's Climate and Energy Fund (Klima- und Energiefonds) for the Grate Advance Project (FFG number 852048) within the framework of the 9<sup>th</sup> Joint Call of ERANET Bioenergy and the Multi Fuel Low Emission project (FFG number 858771) within the 3<sup>rd</sup> call of the Energy Research Program as well of the European Union's Horizon 2020 Research and Innovation Programme under grant agreement number 731101 (BRISK II) are gratefully acknowledged.

## References

- [1] Bioenergy Europe. Statistical Report 2019. Report Bioenergy Landscape; 2019. ; [accessed on 10.01.2020].
- [2] International Energy Agency (IEA). Renewables 2018 – Analysis and forecast to 2023; 2018. <https://www.iea.org/renewables2018/> [accessed on 10.01.2020].
- [3] Bioenergy Europe. Statistical Report 2019. Report Biomass for Heat; 2019. <https://bioenergyeurope.org/statistical-report.html> [accessed on 10.01.2020].
- [4] Nussbaumer T. Combustion and co-combustion of biomass: fundamentals, technologies, and primary measures for emission reduction. *Energy Fuels* 2003;17(6):1510–21.
- [5] Nussbaumer T. Aerosols from Biomass Combustion. Technical report on behalf of the IEA. Bioenergy Task 2017;32.
- [6] Feldmeier S, Wopienka E, Schwarz M, Schön C, Pfeifer C. Applicability of fuel indexes for small-scale biomass combustion technologies, Part 2: TSP and NOx emissions. *Energy Fuels* 2019;33(11):11724–30.
- [7] Kelz J, Brunner T, Obernberger I. Emission factors and chemical characterisation of fine particulate emissions from modern and old residential biomass heating systems determined for typical load cycles. *Environ Sci Eur* 2012;24(1):11.
- [8] Chapela S, Porteiro J, Garabatos M, Patiño D, Gómez MA, Míguez JL. CFD study of fouling phenomena in small-scale biomass boilers: experimental validation with two different boilers. *Renewable Energy* 2019;140:552–62.
- [9] Sommersacher P, Brunner T, Obernberger I. Fuel indexes: a novel method for the evaluation of relevant combustion properties of new biomass fuels. *Energy Fuels* 2011;26(1):380–90.
- [10] Zeng T, Weller N, Pollex A, Lenz V. Blended biomass pellets as fuel for small scale combustion appliances: influence on gaseous and total particulate matter emissions and applicability of fuel indices. *Fuel* 2016;184:689–700.
- [11] Vassilev SV, Baxter D, Andersen LK, Vassileva CG. An overview of the chemical composition of biomass. *Fuel* 2010;89(5):913–33.
- [12] Niu Y, Tan H, Hui SE. Ash-related issues during biomass combustion: Alkali-induced slagging, silicate melt-induced slagging (ash fusion), agglomeration, corrosion, ash utilization, and related countermeasures. *Prog Energy Combust Sci* 2016;52:1–61.
- [13] Werkelin J, Skrifvars BJ, Zevenhoven M, Holmbom B, Hupa M. Chemical forms of ash-forming elements in woody biomass fuels. *Fuel* 2010;89(2):481–93.
- [14] Van Lith SC, Alonso-Ramírez V, Jensen PA, Frandsen FJ, Glarborg P. Release to the gas phase of inorganic elements during wood combustion. Part 1: development and evaluation of quantification methods. *Energy Fuels* 2006;20(3):964–78.
- [15] Van Lith SC, Jensen PA, Frandsen FJ, Glarborg P. Release to the gas phase of inorganic elements during wood combustion. Part 2: influence of fuel composition. *Energy Fuels* 2008;22(3):1598–609.
- [16] Johansen JM, Jakobsen JG, Frandsen FJ, Glarborg P. Release of K, Cl, and S during pyrolysis and combustion of high-chlorine biomass. *Energy Fuels* 2011;25(11):4961–71.
- [17] Frandsen FJ. Quantification of Release of Critical Elements, Formation of Fly Ash and Aerosols: Status on Current Understanding and Research Needs. 11th European Conference on Industrial Furnaces and Boilers (INFUB11). 2017.
- [18] Ma T, Fan C, Hao L, Li S, Jensen PA, Song W, et al. Biomass ash induced agglomeration in fluidized bed. Part 2: Effect of potassium salts in different gas composition. *Fuel Process Technol* 2018;180:130–9.
- [19] Anicic B, Lin W, Dam-Johansen K, Wu H. Agglomeration mechanism in biomass fluidized bed combustion–reaction between potassium carbonate and silica sand. *Fuel Process Technol* 2018;173:182–90.
- [20] Hupa M, Karlström O, Vainio E. Biomass combustion technology development—It is all about chemical details. *Proc. Combust. Instit.* 2017;36(1):113–34.
- [21] Saleh SB, Flensburg JP, Shoulaifar TK, Sárossy Z, Hansen BB, Eggsgaard H, et al. Release of chlorine and sulfur during biomass torrefaction and pyrolysis. *Energy Fuels* 2014;28(6):3738–46.
- [22] Díaz-Ramírez M, Frandsen FJ, Glarborg P, Sebastián F, Royo J. Partitioning of K, Cl, S and P during combustion of poplar and brassica energy crops. *Fuel* 2014;134:209–19.
- [23] Davidsson KO, Stojkova BJ, Pettersson JBC. Alkali emission from birchwood particles during rapid pyrolysis. *Energy Fuels* 2002;16(5):1033–9.
- [24] Jensen PA, Frandsen FJ, Dam-Johansen K, Sander B. Experimental investigation of the transformation and release to gas phase of potassium and chlorine during straw pyrolysis. *Energy Fuels* 2000;14(6):1280–5.
- [25] Knudsen JN, Jensen PA, Dam-Johansen K. Transformation and release to the gas phase of Cl, K, and S during combustion of annual biomass. *Energy Fuels* 2004;18(5):1385–99.
- [26] Okuno T, Sonoyama N, Hayashi JI, Li CZ, Sathe C, Chiba T. Primary release of alkali and alkaline earth metallic species during the pyrolysis of pulverized biomass. *Energy Fuels* 2005;19(5):2164–71.
- [27] Sonoyama N, Okuno T, Mašek O, Hosokai S, Li CZ, Hayashi JI. Interparticle desorption and re-adsorption of alkali and alkaline earth metallic species within a bed of pyrolyzing char from pulverized woody biomass. *Energy Fuels* 2006;20(3):1294–7.
- [28] Liu WJ, Li WW, Jiang H, Yu HQ. Fates of chemical elements in biomass during its pyrolysis. *Chem Rev* 2017;117(9):6367–98.
- [29] Olsson JG, Jäglid U, Pettersson JB, Hald P. Alkali metal emission during pyrolysis of biomass. *Energy Fuels* 1997;11(4):779–84.
- [30] Bostrom D, Skoglund N, Grimm A, Boman C, Ohman M, Brostrom M, et al. Ash transformation chemistry during combustion of biomass. *Energy Fuels* 2011;26(1):85–93.
- [31] Gehrig M, Jaeger D, Pelz SK, Weissinger A, Groll A, Thorwarth H, et al. Influence of firebed temperature on inorganic particle emissions in a residential wood pellet boiler. *Atmos Environ* 2016;136:61–7.
- [32] Fatehi H, He Y, Wang Z, Li ZS, Bai XS, Aldén M, et al. LIBS measurements and numerical studies of potassium release during biomass gasification. *Proc Combust Inst* 2015;35(2):2389–96.
- [33] Zhang ZH, Song Q, Alwahabi ZT, Yao Q, Nathan GJ. Temporal release of potassium from pinewood particles during combustion. *Combust Flame* 2015;162(2):496–505.
- [34] Fatehi H, Li ZS, Bai XS, Aldén M. Modeling of alkali metal release during biomass pyrolysis. *Proc Combust Inst* 2017;36(2):2243–51.
- [35] Sommersacher P, Kienzl N, Brunner T, Obernberger I. Simultaneous online determination of S, Cl, K, Na, Zn, and Pb release from a single particle during biomass combustion. Part 1: Experimental setup-implementation and evaluation. *Energy Fuels* 2015;29(10):6734–46.
- [36] Sommersacher P, Kienzl N, Brunner T, Obernberger I. Simultaneous online determination of S, Cl, K, Na, Zn, and Pb release from a single particle during biomass combustion. Part 2: results from test runs with spruce and straw pellets. *Energy Fuels* 2016;30(4):3428–40.
- [37] Sommersacher P, Kienzl N, Hochenauer C. Online determination of the release of S, Cl, K, Na, Zn and Pb during combustion of a single Miscanthus pellet. In proceedings of the 26th Impacts of Fuel Quality on Power Production, Prague, Czech Republic; 2016.
- [38] Anca-Couce A, Zobel N. Numerical analysis of a biomass pyrolysis particle model: solution method optimized for the coupling to reactor models. *Fuel* 2012;97:80–8.
- [39] Anca-Couce A, Sommersacher P, Shiehnejadhesar A, Mehrabian R, Hochenauer C, Scharler R. CO/CO2 ratio in biomass char oxidation. *Energy Proc* 2017;120:238–45.
- [40] Anca-Couce A, Caposciutti G, Gruber T, Kelz J, Bauer T, Hochenauer C, et al. Single large wood log conversion in a stove: Experiments and modelling. *Renewable Energy* 2019;143:890–7.
- [41] Anca-Couce A, Sommersacher P, Scharler R. Online experiments and modelling with a detailed reaction scheme of single particle biomass pyrolysis. *J Anal Appl Pyrol* 2017;127:411–25.
- [42] NIST-JANAF Thermochemical Tables. NIST Standard Reference Database 13. <https://janaf.nist.gov/> [last accessed on 29.02.2020].
- [43] Olwa J, Öhman M, Esbjörn P, Boström D, Okure M, Kjellström B. Potassium retention in updraft gasification of wood. *Energy Fuels* 2013;27(11):6718–24.
- [44] Novakovic A, van Lith SC, Frandsen FJ, Jensen PA, Holgersen LB. Release of potassium from the systems K – Ca – Si and K – Ca – P. *Energy Fuels* 2009;23(7):3423–8.